Eyewall Contraction, Breakdown and Reformation in a Landfalling Typhoon

Chun-Chieh Wu, Kun-Hsuan Chou, and Hsiu-Ju Cheng
Department of Atmospheric Sciences, National Taiwan University, Taipei, Taiwan

Yuqing Wang
International Pacific Research Center, School of Ocean and Earth Science and Technology, University of Hawaii at Manoa, Honolulu, USA

Received 30 April 2003; revised 26 June 2003; accepted 24 July 2003; published 5 September 2003.

[1] The interesting eyewall evolution of Typhoon Zeb before, during, and after its landfall at Luzon was documented from both the satellite observation and numerical simulation. It is proposed that the terrain plays a critical role in leading to such evolution: first the eyewall contraction just before landfall, a following breakdown, and then the eyewall reformation after the storm returned to the ocean. Further studies of the physical mechanisms responsible for such eyewall evolution shall improve both our understanding of and the skill in predicting the structure and intensity changes of tropical cyclones in general and landfalling ones in particular. *INDEX TERMS:* 3322 Meteorology and Atmospheric Dynamics: Land/atmosphere interactions; 3337 Meteorology and Atmospheric Dynamics: Numerical modeling and data assimilation; 3339 Meteorology and Atmospheric Dynamics: Ocean/atmosphere interactions (0312, 4504); 3374 Meteorology and Atmospheric Dynamics: Tropical meteorology. **Citation:** Wu, C.-C., K.-H. Chou, H.-J. Cheng, and Y. Wang, Eyewall Contraction, Breakdown and Reformation in a Landfalling Typhoon, *Geophys. Res. Lett.*, *30*(17), 1887, doi:10.1029/2003GL017653, 2003.

1. Introduction

[2] The eyewall of a tropical cyclone (TC) is constituted by deep clouds surrounding the eye, which on the contrary contains only light winds and almost no precipitation. The most severe weather, such as maximum winds and torrential rains, occurs in the eyewall. It is also generally believed that the evolution of the eyewall is responsible for the intensity change of a TC. Therefore, the evolution of the eyewall has always been an intriguing issue in TC thermodynamics and dynamics. As shown by *Shapiro and Willoughby* [1982], some interesting eyewall features include: The contraction of the radius of maximum wind; the convective updrafts entraining air outward from the eye, the area encompassed by the convective ring, which leads to subsidence, adiabatic warming, and pressure falls in the eye; the outer eyewall acting as a barrier to the boundary layer inflow, which reduces the mass convergence, as well as the updraft in the inner eyewall, and thus weakens the storm.

[3] Meanwhile, the replacement of concentric eyewalls [*Willoughby et al.*, 1982; *Willoughby and Black*, 1996] and the horizontal (potential) vorticity mixing between the eye and the eyewall [*Kossin and Eastin*, 2001] can lead to distinct changes in the kinematic and thermodynamic structure of the eye and eyewall. *Knaff et al.* [2003] also described the role of asymmetric mixing of the eye and eyewall components of the storms in the formation of the annular hurricanes, which compared to greater populations of tropical cyclones are distinctly more axisymmetric with circular eyes surrounded by a nearly uniform ring of deep convection and a curious lack of deep convective features outside the ring. On the other hand, the dynamical instability can result in the formation of mesovortices and the polygonal eyewall structure [*Schubert et al.*, 1999; *Kossin and Schubert*, 2001], while the presence of asymmetric counter-propagating convectively coupled vortex Rossby waves can interact with the mean vortex and cause intensity change [*Montgomery and Kallenbach*, 1997; *Wang*, 2002a; *Wang*, 2002b].

[4] Here another interesting eyewall evolutionary process is documented. As illustrated by the satellite images during the period when Typhoon Zeb (1998) devastated Luzon, its eyewall shrank before landfall (cf. Figure 1a, 1b), and then its inland portion disappeared possibly due to the terrain effect and the covering of the high cloud (Figure 1c). A few hours later, a wider eyewall reformed (Figure 1d, 1e) as Zeb left Luzon and the eyewall contracted again as it moved along the east coast of Taiwan (Figure 1f). Similar features have also been observed in other storms, such as Typhoons Dan (1999) and Imbudo (2003) over Luzon, and Hurricane Gilbert (1987) over Yucatan, but they have never been documented and investigated in detail in the literature. In this paper we present the first successful simulation of such eyewall evolution using the high-resolution numerical model MM5 (the fifth generation National Center for Atmospheric Research-Pennsylvania State University Mesoscale Model).

2. Results

[5] The MM5 with triply nested meshes of 45/15/5-km resolution was used to perform a 72-h simulation, starting from 0000 UTC 13 October 1998. The initial and lateral boundary conditions are based on the European Centre for Medium-range Weather Forecasts (ECMWF) global analysis, with the fixed sea surface temperature (SST) taken from the weekly mean SST available at National Centers for Environmental Prediction (NCEP). The model initialization and vortex bogusing are based on the method described in *Wu et al.* [2002]. Note that ideally a higher-resolution simulation (1.7-km) may produce a more detailed eyewall structure. Nevertheless we believe that the 5-km resolution employed in this work can capture the major eyewall

0094-8276/03/2003GL017653$05.00

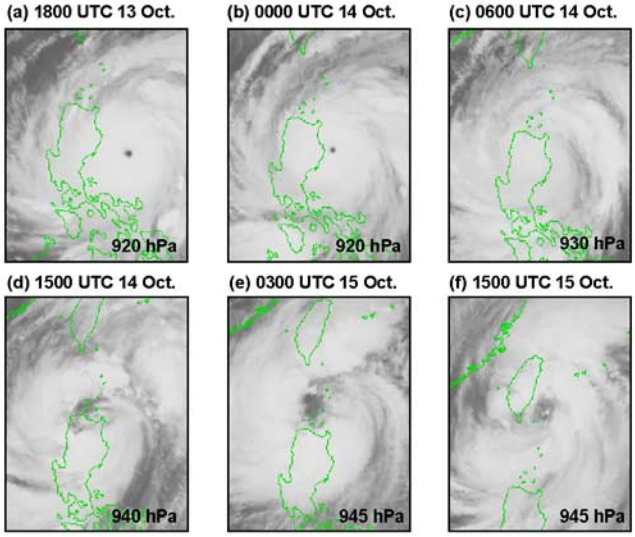

Figure 1. GMS satellite IR images: (a) 1800 UTC 13 Oct. 1998; (b) 0000 UTC 14 Oct.; (c) 0600 UTC 14 Oct.; (d) 1500 UTC 14 Oct.; (e) 0300 UTC 15 Oct.; (f) 1500 UTC 15 Oct. The central minimum sea-level pressure from the best-track analysis of Central Weather Bureau of Taiwan is indicated in the lower-right side of each panel.

evolution processes, while eddy mixing is well dominant over the artificial diffusion processes [cf. *Kossin and Schubert*, 2003].

[6] Except for the northward deviation in the incipient 18 h, the track of Zeb (Figure 2) is reasonably well simulated, with an error of 15, 23, and 146 km, for 24, 48 and 72 h, respectively. The tendency of the intensity change is also well simulated though the model intensity is somewhat weaker with the minimum central sea-level pressure higher than the best-track analysis by about 20 hPa (see the values of the storm's central minimum sea-level pressure indicated in Figures 1 and 3).

[7] The main features of eyewall contraction, breakdown and reformation processes during the period when Zeb was near Luzon are also well simulated. As shown in Figure 3a and 3b, the model-estimated radar reflectivity at 700 hPa indicates that the eye shrinks during the first 12–24 h as Zeb approaches Luzon, similar to the eyewall contraction of Hurricane Andrew (1992) before its landfall at Miami [*Willoughby and Black*, 1996]. Unlike the satellite images in Figure 1c, the eyewall remains complete during the first few hours after Zeb's landfall at Luzon (Figure 3c). The eyewall then gradually breaks down while the inner rainband becomes less organized in the next few hours (Figure 3d). Finally, interestingly enough, the outer rainband reorganizes and a larger eyewall forms (Figure 3e) when Zeb re-enters the warm ocean. The eyewall contracts again (Figure 3f) as Zeb re-intensifies while moving toward the east coast of Taiwan. The simulated evolution of the eyewall is consistent with the satellite observations as shown in Figure 1.

[8] The radius of maximum mean tangential wind (RMTW) at $\sigma = 0.995$ (the lowest model level) reduces from 45 km at 12 h to 38 km at 24 h before the eyewall makes landfall (Figure 4a). The maximum mean azimuthal flow also weakens from 44 to 35 m s^{-1}. Apparently, such eyewall contraction with decreasing intensity is different from the finding of eyewall contraction with strengthening intensity before Andrew (1992) made landfall near Miami [*Willoughby and Black*, 1996]. Such a difference is likely to result from the stronger dissipation and drying effect from the terrain and topography as Zeb approached and made landfall at Luzon. Another notable feature is the weakening of the outer circulation (e.g., the radius of 20-m s^{-1} wind decreases from 160 to 130 km) during this period.

[9] Such a weakening tendency continues as far as Zeb is about to leave Luzon at 34h. The RMTW keeps increasing during 34 and 44 h with a slight intensity increase from 21 to 25 m s^{-1}. Interestingly, from 46 to 60 h, Zeb re-intensifies quickly with the maximum azimuthal wind increasing from 25 to 39 m s^{-1} while the RMTW decreases with time from 90 to 75 km (i.e., the eyewall contracts again). All the above-mentioned processes are generally consistent with the evolution of the mean radial inflow (Figure 4b), with the radius of the maximum radial flow slightly greater than RMTW.

[10] To highlight the asymmetric component of the eyewall, the radius-time Hovmöller diagram of total wind speed at $\sigma = 0.995$ zonally across the typhoon center from 1200 UTC 13 to 1500 UTC 15 October 1998 (model hour from 12 to 63 h) is also analyzed (figure not shown). During the period before Zeb made landfall (Stage I, see Figure 4), the strongest wind is located in the west portion, i.e., the landward side of the storm, similar to that in Hurricane Andrew [*Willoughby and Black*, 1996]. The wind speed decreases as Zeb makes landfall (Stage II), then the region of maximum wind becomes less obvious as Zeb moves further inland (Stage III). The bigger eye reforms as Zeb re-enters the ocean (Stage IV), and shrinks again with maximum wind to the east of the storm center, i.e., the right-hand side relative to the storm motion.

[11] To emphasize the difference of the storm structure at different stages (see Figure 4), Figure 5 shows the time, azimuthal and vertical averages calculated and presented at the four stages. The maximum boundary-layer (averaged between $\sigma = 0.995$ and 0.91) tangential wind (V_t) of 55 m s^{-1} is present at Stage I, with a RMTW of 50 km (Figure 5a). The RMTW decreases to 45 km at Stage II, while its strongest V_t decreases to 42 m s^{-1}. At Stage III the whole curve flattens with no obvious RMTW, an indicator of the obscure eyewall structure. The eyewall reorganizes at

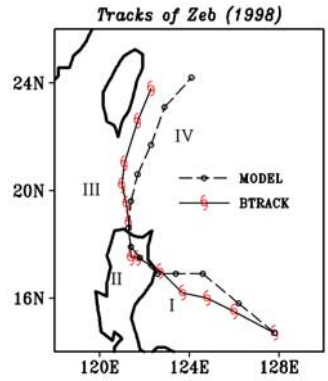

Figure 2. 72-h best tracks (indicated with typhoon symbol) and model tracks (indicated with the solid dot) of Typhoon Zeb (1998), shown at 6-h interval from 0000 UTC 13 Oct. to 0000 UTC 16 Oct. 1998.

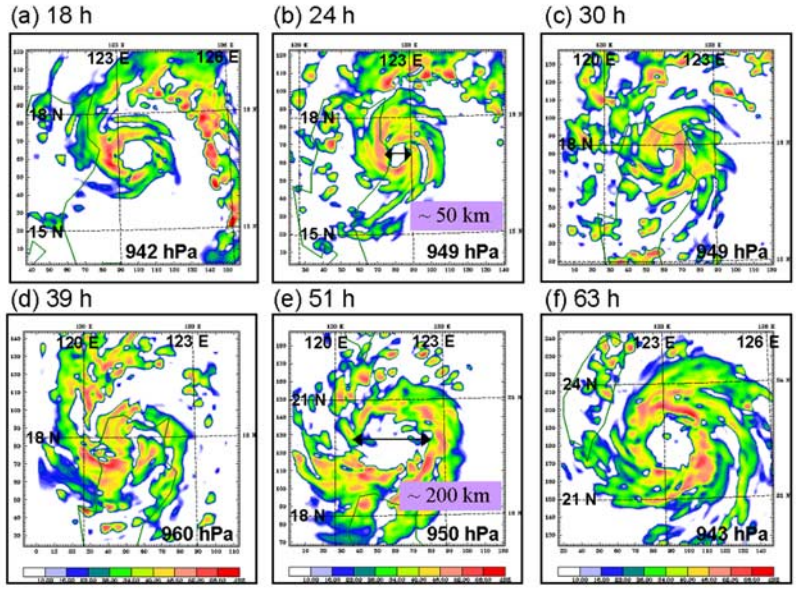

Figure 3. The same time as Figure 1, but for model-simulated radar reflectivity (dBZ) at 700 hPa: (a) 18h; (b) 24h; (c) 30h; (d) 39h; (e) 51h; (f) 63h. The model storm's central minimum sea-level pressure is indicated in the lower-right side of each panel.

Stage IV, with a larger RMTW of 77 km, and maximum V_t of 47 m s^{-1}.

[12] The distribution of mean boundary-layer radial wind (Figure 5b) shows that the maximum radial inflow (V_r) of 22 m s^{-1} is located at the radius of 63 km at Stage I. The maximum V_r decreases to 16 m s^{-1} at 73 km at Stage II, and further weakens to 13 m s^{-1} while extending further outward at 165 km at Stage III. At Stage IV, the maximum V_r increases to 18 m s^{-1}, while its associated radius shrinks to 120 km.

[13] The low-level (averaged between σ = 0.995 and 0.91) potential vorticity (PV) profiles (Figure 5c) show the typical PV ring distribution, with the maximum slightly inward of the RMTW. The maximum PV value decreases from 20, 18, to 13 PV unit (1 PVU = 1 x 10^{-6} $m^2 s^{-1} K kg^{-1}$) from Stages I, II to III. At Stage IV, a much weaker PV maximum (9 PVU) is present off the center. Such PV evolution is similar to that described in *Kossin and Eastin* [2001] in the PV mixing between the eye and the eyewall, though in our study the terrain plays an extra role in leading to the PV mixing while weakening.

[14] The distribution of the middle-level (averaged between σ = 0.625 and 0.425) vertical velocity (w) is also noteworthy (see Figure 5d). The peak w reaches 1 m s^{-1}, and is located slightly outside maximum of V_t at Stage I, and then reduces to 0.7 m s^{-1} at a slightly smaller radius at Stage II. The w profile flattens significantly at Stage III, with a maximum w of 0.3 m s^{-1} at a radius twice as large as the previous stage. It then increases to 0.6 m s^{-1} at a radius consistent with that of V_t as shown in Figure 5a.

[15] The evolution of the warm core structure is also obvious from the potential temperature profile in the middle troposphere (Figure 5e). The strength of the middle-layer mean warm core structure reduces quickly from Stage I to III, and then increases again at Stage IV. Finally the relative humidity (RH, Figure 5f) shows the lowest value of 50% in the eye at Stage I, then increasing dramatically to a value of 84% (95%) at Stage II (III), probably as a result of the increased mixing and weakening of the eyewall when Zeb is over the terrain. The RH in the eye drops to 74% again as its eyewall reforms at a larger radius at Stage IV.

3. Summary

[16] In this study, we present a preliminary numerical simulation of the eyewall evolution of Typhoon Zeb as it

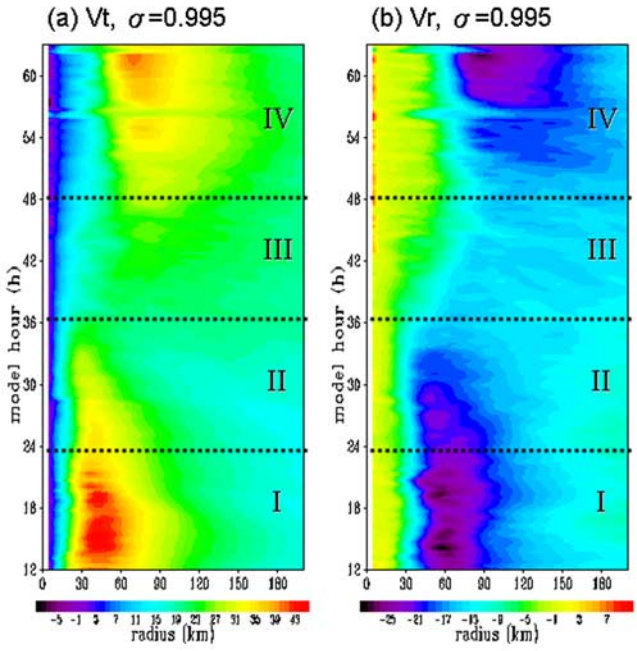

Figure 4. Radius-time Hovmöller diagram of azimuthal average at σ = 0.995 from 1200 UTC 13 to 1800 UTC 15 Oct. 1998 (model hour from 12 to 63 h): (a) tangential wind (m s^{-1}); (b) radial wind (m s^{-1}). The dotted lines show the time when Zeb makes landfall (24 h), leaves Luzon (36 h), and redevelops (48 h), respectively. (I), (II), (III) and (IV), as separated by the dotted lines, indicate the four different temporal stages for time-average calculation.

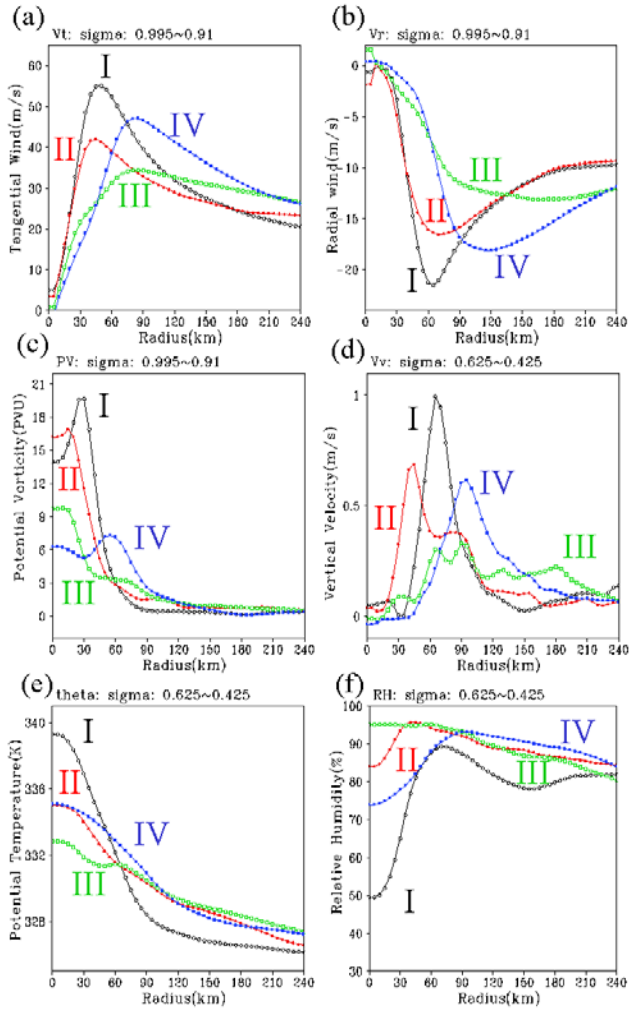

Figure 5. Time, azimuthal and vertical average of (a) tangential wind (V_t, m s^{-1}) as a function of radius (in km) from the storm center at σ = 0.995–0.91; (b) radial wind (V_r, m s^{-1}); (c) potential vorticity PV, PVU); (d) vertical velocity (w, m s^{-1}) atσ = 0.625–0.425; (e) potential temperature (θ, K); and (f) relative humidity (RH, %). Each curve represents time average at different stages: I (black), II (red), III (green), and IV (blue).

interacted with the terrain of Luzon using MM5. The main features of eyewall contraction, breakdown and reformation during the period when Zeb approached, made landfall at, and left Luzon are well simulated. In particular, the thermodynamic and kinematic fields at different stages of the eyewall evolution are analyzed. It is shown that the eyewall contraction occurred due to an increased inflow in the coastal region before landfall, which was accompanied by the continual weakening of the storm. The weakening of the storm, the presence of the ambiguous eyewall, and its quasi-breakdown after landfall was likely due to both the terrain dissipation and the water vapor cutoff, while the outer circulation was still less affected. Finally the outer circulation reorganized and led to the formation of the new large eyewall and its subsequent contraction as Zeb left Luzon.

[17] The results shown here may stimulate further detailed investigation, thus enhancing our understanding of interactions among the TC eyewall and its larger circulation, the underlying surface and terrain and their effect on storm structure and intensity changes. We propose that such eyewall evolution may often occur when a storm encounters terrain with the size comparable to the vortex size. However, some more questions remain unanswered.

[18] (i) What are the key parameters determining the evolutionary processes of a landfalling TC?

[19] (ii) How does the eddy (the asymmetric component) interact with the mean flow (the symmetric component), resulting in the storm intensity change?

[20] (iii) What kind of roles do the terrain, surface drag, and ocean heat flux play relative to those eyewall processes?

[21] To answer these questions, we plan to conduct comprehensive budget analyses to evaluate the interaction between the eddy and the mean flow and also to perform more numerical experiments with different setups of the surface condition (such as terrain height and the prescribed surface latent heat flux) to gain better insight into the aforementioned questions. It is believed that further work can provide a better understanding of such special eyewall evolution processes as the TC makes landfall at certain terrains and reach a conceptual model to improve the forecast of severe weather in landfalling TCs.

[22] **Acknowledgments.** We thank Jim Kossin for his helpful comments. The work is supported through the National Science Council of Taiwan by Grant NSC91-2119-M-002-032. Yuqing Wang acknowledges the support by U.S. Office of Naval Research under Grant N00014-021-0532 and the National Science Foundation under Grant ATM-0119490.

References

Knaff, J. K., J. P. Kossin, and M. DeMaria, Annular hurricanes, *Wea. Forecasting*, *18*, 204–223, 2003.

Kossin, J. P., and M. D. Eastin, Two Distinct regimes in the kinematic and thermodynamic structure of the hurricane eye and eyewall, *J. Atmos. Sci.*, *58*, 1079–1090, 2001.

Kossin, J. P., and W. H. Schubert, Mesovortices, polygonal flow patterns, and rapid pressure falls in hurricane-like vortices, *J. Atmos. Sci.*, *58*, 2196–2209, 2001.

Kossin, J. P., and W. H. Schubert, Diffusion versus advective rearrangement of a circular vortex sheet, *J. Atmos. Sci.*, *60*, 586–589, 2003.

Montgomery, M. T., and R. J. Kallenbach, A theory for vortex Rossby-waves and its application to spiral bands and intensity changes in hurricanes, *Q. J. R. Meteorol. Soc.*, *123*, 435–465, 1997.

Schubert, W. H., M. T. Montgomery, R. K. Taft, T. A. Guinn, S. R. Fulton, J. P. Kossin, and J. P. Edwards, Polygonal eyewalls, asymmetric eye contraction, and potential vorticity mixing in hurricanes, *J. Atmos. Sci.*, *56*, 1123–1197, 1999.

Shapiro, L. J., and H. E. Willoughby, The response of balanced hurricanes to local sources of heat and momentum, *J. Atmos. Sci.*, *39*, 378–394, 1982.

Wang, Y., Vortex Rossby waves in a numerically simulated tropical cyclone. Part I: Overall structure, potential vorticity, and kinetic energy budgets, *J. Atmos. Sci.*, *59*, 1213–1238, 2002a.

Wang, Y., Vortex Rossby waves in a numerically simulated tropical cyclone. Part II: The role in tropical cyclones structure and intensity changes, *J. Atmos. Sci.*, *59*, 1239–1262, 2002b.

Willoughby, H. E., J. A. Clos, and M. G. Shoreibah, Concentric eyewalls, secondary wind maximum, and the evolution of the hurricane vortex, *J. Atmos. Sci.*, *39*, 395–411, 1982.

Willoughby, H. E., and P. G. Black, Hurricane Andrew in Florida: Dynamics of a disaster, *Bull. Am. Meteorol. Soc.*, *77*, 543–549, 1996.

Wu, C.-C., T.-H. Yen, Y.-H. Kuo, and W. Wang, Rainfall simulation associated with Typhoon Herb (1996) near Taiwan. Part I: The topographic effect, *Wea. and Forecasting*, *17*, 1001–1015, 2002.

C.-C. Wu, Department of Atmospheric Sciences, National Taiwan University, No. 1, Sec. 4, Roosevelt Rd., Taipei, 106, Taiwan. (cwu@typhoon.as.ntu.edu.tw)

K.-H. Chou and H.-J. Cheng, Department of Atmospehric Sciences, National Taiwan University, Taiwan. (cwujou@typhoon.as.ntu.edu.tw; cwucheng@typhoon.as.ntu.edu.tw)

Y. Wang, International Pacific Research Center, School of Ocean and Earth Science and Technology, University of Hawaii at Manoa, Honolulu, USA. (yqwang@soest.hawaii.edu)